

Chapter 1

DISCRETE AND CONTINUOUS MODELS

1.1 Coexistence of the Dynamical Order and Chaos

Hamiltonian systems are carriers of chaos. With minimal restrictions, the phase space of an arbitrary dynamic Hamiltonian system contains regions where motion is accompanied by a mixing of trajectories in the phase space. The analytical and graphic methods currently available are not good enough to capture the dynamics, which can be either chaotic or regular. More or less successful methods of studying dynamics exist only for systems which do not have more than two degrees of freedom. A system with N degrees of freedom is characterised by N pairs of the generalised co-ordinates (q_1, \dots, q_N) and momentums (p_1, \dots, p_N) , which satisfy the Hamiltonian equation of motion

$$\dot{p}_i = -\frac{\partial H}{\partial q_i}, \quad \dot{q}_i = \frac{\partial H}{\partial p_i}, \quad (i = 1, \dots, N) \quad (1.1.1)$$

where

$$H(p, q) \equiv H(p_1, q_1, \dots, p_N, q_N) \quad (1.1.2)$$

is the Hamiltonian of the system. The Hamiltonian depends on time and we will only consider the situation when this dependence is time-periodic with period

$$T = 2\pi/\nu. \quad (1.1.3)$$

That is, if $H = H(p, q; t)$, then

$$H(p, q; t + T) = H(p, q, t). \quad (1.1.4)$$

We define system (1.1.4) as having $N + 1/2$ degrees of freedom since the time variable is an additional canonical variable.

Chaotic trajectories occur in $N = 1 1/2$ degrees of freedom system of the general type. The trajectories of the system can be displayed in a two-dimensional phase plane such that the set of points $(p(t_n), q(t_n))$ correspond to the time instants $t_n = t_0 + nT$. This method of representing a trajectory is known as the Poincaré map. In fact, one sometimes find that

$$(p_{n+1}, q_{n+1}) = \hat{T}(p_n, q_n) \quad (1.1.5)$$

where

$$p_n \equiv p(t_n), \quad q_n \equiv q(t_n)$$

and \hat{T} is a shift operator by time T . The Poincaré map (1.1.5) simplifies the original problem (1.1) which consists of an integration of a part of the motion.

Despite the low dimensionality of such systems with chaos, many models have been developed and thus merit discussion. This chapter presents some of the more common types of the map \hat{T} . This discussion is also taken up in the following chapters.

Prior to a systematic description of the different models, it is worthwhile to present a view of the plane for a typical system with $1 1/2$ degrees of freedom and bounded motion. A schematic picture is presented in Fig. 1.1.1. The dots belong to a trajectory in the domain of chaotic dynamics (stochastic sea) and the curves are closures at the Poincaré map for quasi-periodic (non-chaotic) motion in the so-called islands. In reality, isolated domains of chaotic motion also exist inside the islands. A magnification of an island will show that it resembles the main picture in Fig. 1.1.1, thus confirming the complexity of chaotic dynamics.

The coexistence of both regions of stable dynamics and chaos in the phase space is one of the most striking and wonderful discoveries ever made. It enables one to analyse the onset of chaos and the appearance of the minimal region of chaos. Although not much is known about this field, it is nevertheless evident that a seed of chaos (a so-called stochastic layer) exists which replaces the vicinity of destroyed separatrices.

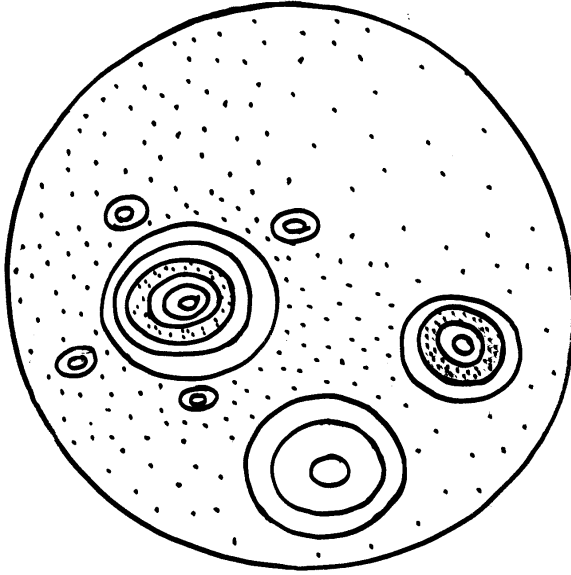


Fig. 1.1.1. Structure of the phase space.

1.2 The Standard Map (Kicked Rotator)

This map, also referred to as the Chirikov-Taylor map, emerges in many physical problems. It offers a simplified model of the onset of chaos by retaining the typical complex features of the problem.

The Hamiltonian of a system which can be described by the standard map is expressed as

$$H = \frac{1}{2}I^2 - K \cos \theta \sum_{n=-\infty}^{\infty} \delta\left(\frac{t}{T} - n\right). \quad (1.2.1)$$

It defines the system with an unperturbed Hamiltonian,

$$H_0 = \frac{1}{2}I^2, \quad (1.2.2)$$

which is affected by a periodic sequence of kicks (δ -pulses) with the period

$$T = 2\pi/\nu. \quad (1.2.3)$$

Expression (1.2.2) corresponds either to a particle's free motion, $I = p$, $\theta = x$, or to a free rotator when the variable θ is cyclic, that is, $\theta \in (0, 2\pi)$. Let us consider the latter case. By using the identity

$$\sum_{n=-\infty}^{\infty} \delta\left(\frac{t}{T} - n\right) = \sum_{n=-\infty}^{\infty} \cos\left(2\pi n \frac{t}{T}\right), \quad (1.2.4)$$

we rewrite (1.2.1) in the following form:

$$H = \frac{1}{2}I^2 - K \cos \theta \sum_{m=-\infty}^{\infty} \cos m\nu t. \quad (1.2.5)$$

The Hamiltonian (1.2.5) can also be considered as a particular case of a more general Hamiltonian,

$$H = \frac{1}{2}p^2 + \sum_m V_m \cos(k_m x - \omega_m t), \quad (1.2.6)$$

when

$$k_m = 1(\forall m), \quad V_m = V_0 = -K(\forall m), \quad \omega_m = m\nu$$

and the sum in (1.2.6) is performed over $m \in (-\infty, \infty)$. Thus, the Hamiltonian (1.2.1) corresponds to a particle motion in a periodic wave packet with an infinite number of harmonics of equal amplitude.

The equations of motion derived from (1.2.1) have the form

$$\begin{aligned} \dot{I} &= -K \sin \theta \sum_{n=-\infty}^{\infty} \delta\left(\frac{t}{T} - n\right) \\ \dot{\theta} &= I. \end{aligned} \quad (1.2.7)$$

Between two δ -functions, $I = \text{const}$ and $\theta = It + \text{const}$. At each step, or kick, represented by the δ -function, the variable θ remains continuous and the action I changes by the value $-K \sin \theta$, which can be obtained by integrating (1.2.7) with respect to time in a small vicinity of the δ -function. If we assume that (I, θ) are the values of the variables just

before the n -th kick, and that $(\bar{I}, \bar{\theta})$ are the same values before the next $(n + 1)$ -th kick, it follows that the map, derived from (1.2.7), is

$$\begin{aligned}\bar{I} &= I - K \sin \theta \\ \bar{\theta} &= \theta + \bar{I},\end{aligned}\tag{1.2.8}$$

which is equivalent to the equations of motion in (1.2.7). Here we shall restrict ourselves to some brief comments on the map (1.2.8) by postponing the main discussion to Chapter 2.¹

For $K = 0$, there is no perturbation and the solution of (1.2.8) is trivial:

$$I_n = \text{const.} = I_0, \quad \theta_n = \theta_0 + nI_0.\tag{1.2.9}$$

It describes the straight line on the phase plane (I, θ) as shown in Fig. 1.2.1(a). The same trajectory can be put either on the torus $I(\text{mod } 2\pi)$, $\theta(\text{mod } 2\pi)$, as shown in Fig. 1.2.1(b), or on the cylinder $I \in (-\infty, \infty)$, $\theta(\text{mod } 2\pi)$. Both ways are equivalent in terms of presenting a trajectory or a phase portrait of system (1.2.8) and their convenience is the only consideration in making such a choice. This situation arises because of the existence of a fundamental domain, $[I \in (0, 2\pi); \theta \in (0, 2\pi)]$, for map (1.2.8). This domain can be either arbitrarily shifted or multiplied by integers in both directions.

For small values of K , one can consider an approximation of (1.2.8) by introducing derivatives instead of finite differences. Hence

$$\frac{dI}{dt} = -\frac{1}{T}K \sin \theta, \quad \frac{d\theta}{dt} = \frac{1}{T}I,\tag{1.2.10}$$

or

$$\frac{d^2\theta}{d(t/T)^2} + K \sin \theta = 0,\tag{1.2.11}$$

¹The standard map was proposed by J. B. Taylor [Ta 69] as a model to study the existence of the invariants of motion in magnetic traps. B. V. Chirikov used a more formal means to obtain the standard map [C 79]. Later, it became clear that the situation described by the standard model occurs in numerous applications on physical systems [see (LiL 93)].

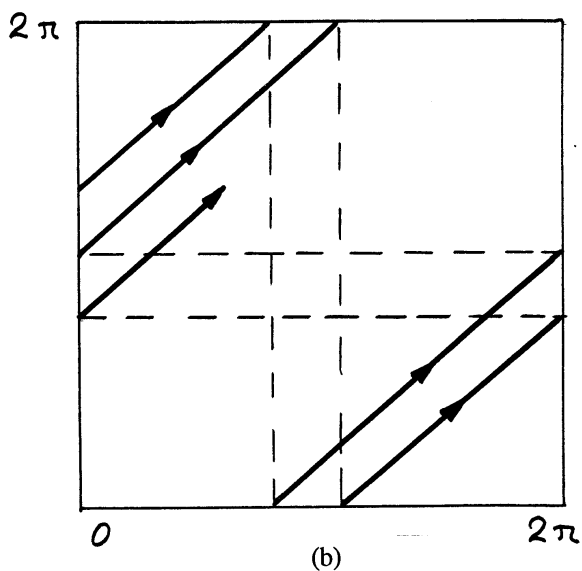
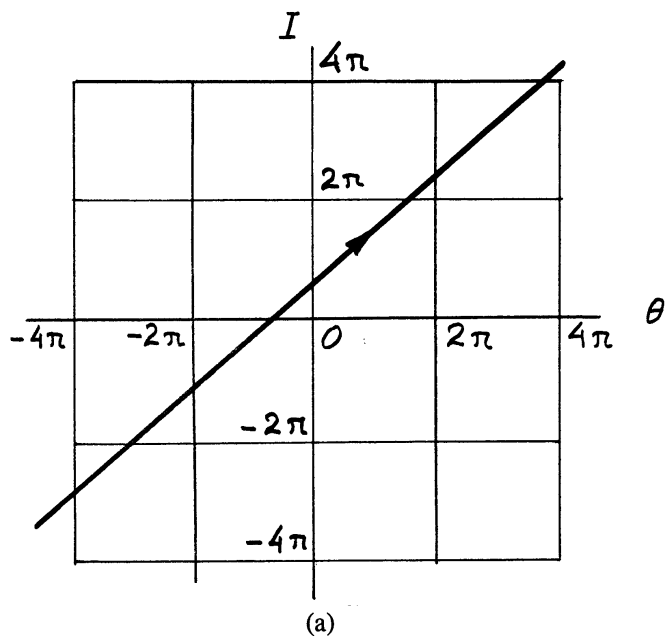
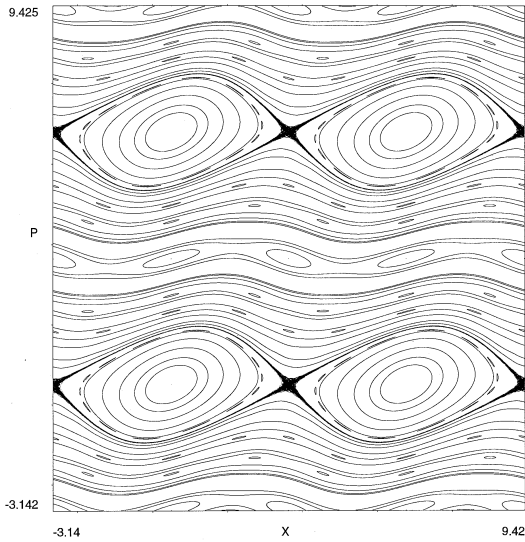
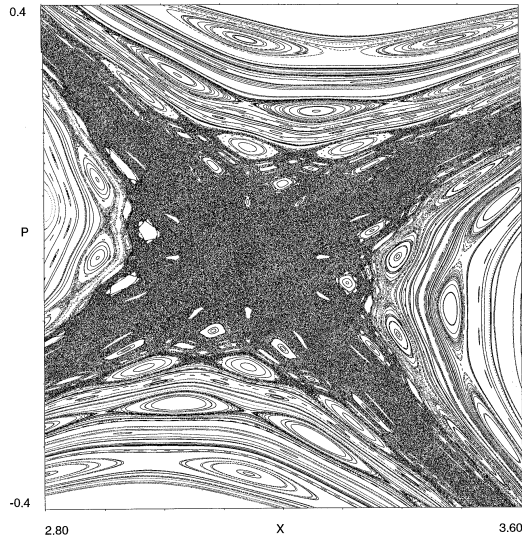


Fig. 1.2.1. A trajectory in: (a) double-periodic phase space; (b) fundamental domain (on the torus).



(a)



(b)

Fig. 1.2.2. The phase portrait of the standard map ($K = 0.5$): (a) part of the phase space 2×2 periods; (b) magnification of an area near the saddle point.

which is the pendulum equation with Hamiltonian

$$H = \frac{1}{T} \left(\frac{1}{2} I^2 - K \cos \theta \right) \quad (1.2.12)$$

and frequency $K^{1/2}$. Up to a constant, the Hamiltonian (1.2.12) coincides with (1.2.5) if we neglect all the terms in the sum except for $m = 0$. This is a very poor approximation, and it can be seen after a comparison between the integrable pendulum phase portrait and that of the original map (1.2.8), as shown in Fig. 1.2.2. We use four elementary fundamental domains to make Fig. 1.2.2 more representative. Such complexity, as well as the variety of trajectory types, cannot be obtained by any known perturbation method. Narrow zones with chaotic trajectories are called stochastic layers. Inside these stochastic layers are islands with nested curves, sub-islands and smaller stochastic layers.

1.3 The Web-Map (Kicked Oscillator)

The web-map is a result of the consideration of particle motion in a constant magnetic field and an electrostatic wave packet propagating perpendicularly to the magnetic field. The Hamiltonian of the system is

$$H = \frac{1}{2} (p^2 + \omega_0^2 x^2) - \frac{\omega_0 K}{T} \cos x \sum_{m=-\infty}^{\infty} \delta \left(\frac{t}{T} - n \right), \quad (1.3.1)$$

where ω_0 is the gyro-frequency and K the dimensionless parameter proportional to the perturbation amplitude. The derivation of the map is similar to that for a standard map.

Consider the equation of motion that follows from (1.3.1):

$$\ddot{x} + \omega_0^2 x = -\frac{\omega_0 K}{T} \cos x \sum_{m=-\infty}^{\infty} \delta \left(\frac{t}{T} - n \right). \quad (1.3.2)$$

It describes a linear oscillator affected by a periodic set of kicks. The model (1.3.2) can be reduced to the standard map (1.2.1) by using only a singular transform: $\omega_0 \rightarrow 0$, $K \rightarrow \infty$, $\omega_0 K = \text{const}$. For any finite K , the results described below cannot be simply considered in the limit

$\omega_0 = 0$, and that makes the kicked-oscillator model independent of the kicked-rotator model. Next, we define

$$x_n = x(t_n - 0), \quad \dot{x}_n = v_n = p_n/m = \dot{x}(t_n - 0) \quad (1.3.3)$$

with the discrete time being $t_n = nT$. From (1.3.2), it follows that, directly by integration,

$$\begin{aligned} x(t_n + 0) &= x(t_n - 0) \\ \dot{x}(t_n + 0) &= \dot{x}(t_n - 0) - K\omega_0 \sin x_n. \end{aligned} \quad (1.3.4)$$

Between two adjacent kicks, the solution of (1.3.2) satisfies the free motion equation,

$$\ddot{x} + \omega_0^2 x = 0,$$

which permits one to express $x_{n+1} = x(t_{n+1} - 0)$, $\dot{x}_{n+1} = \dot{x}(t_{n+1} - 0)$ through $x(t_n + 0)$, $\dot{x}(t_n + 0)$. After applying (1.3.4), we obtain the map

$$\begin{aligned} u_{n+1} &= (u_n + K \sin v_n) \cos \alpha + v_n \sin \alpha \\ v_{n+1} &= -(u_n + K \sin v_n) \sin \alpha + v_n \cos \alpha \end{aligned} \quad (1.3.5)$$

where the following dimensionless variables are introduced:

$$u = \dot{x}/\omega_0, \quad v = -x, \quad \alpha = \omega_0 T. \quad (1.3.6)$$

The map obtained, (1.3.5), is called the web-map for reasons that will soon become clear. Using the complex variable $z = u + iv$, we rewrite the web-map (1.3.5) as

$$z_{n+1} = \left(z_n + K \sin \frac{z - z^*}{2i} \right) e^{i\alpha}, \quad (1.3.7)$$

that is,

$$z_{n+1} = \hat{R}_\alpha (1 + \hat{S}(K)) z_n \quad (1.3.8)$$

where \hat{R}_α is the rotation transform by α and $S(K)$ the shear transform along $\text{Im } z$ with intensity parameter K .²

²The web-map was derived in [ZZSUC 86] and used on different physical problems, including the problem of quasi-crystal symmetry generation [see (ZSUC 91)].

The most interesting case involving map (1.3.5) is that of the resonance between sequences of kicks and oscillator frequency ω_0 . To simplify this condition, consider

$$\alpha = \omega_0 T = 2\pi/q \quad (1.3.9)$$

with an integer q and denote

$$\hat{M}_q = \hat{R}_{2\pi/q} \cdot \hat{S}(K). \quad (1.3.10)$$

Some simple examples of the resonance case (1.3.9) include

$$\begin{aligned} \hat{M}_1: u_{n+1} &= u_n + K \sin v_n, & v_{n+1} &= v_n \\ \hat{M}_2: u_{n+1} &= -u_n - K \sin v_n, & v_{n+1} &= -v_n \\ \hat{M}_2^2: u_{n+2} &= u_n + 2K \sin v_n, & v_{n+2} &= v_n \end{aligned} \quad (1.3.11)$$

which correspond to the operating regimes of the earliest cyclotrons. A more complicated case arises when $q = 4$:

$$\hat{M}_4: u_{n+1} = v_n \quad v_{n+1} = -u_n - K \sin v_n. \quad (1.3.12)$$

It is non-integrable and possesses chaotic trajectories (see Fig. 1.3.1). For small $K \ll 1$ in the first approximation, it is easy to derive

$$\hat{M}_4^4 \approx \hat{M}_H: \begin{aligned} \bar{u} &= u + 2K \sin \bar{v} \\ \bar{v} &= v - 2K \sin u \end{aligned}, \quad (1.3.13)$$

where \hat{M}_H corresponds to the so-called Harper kicked oscillator described by the Hamiltonian

$$H_H = -\frac{1}{2}K \left\{ \cos v + \cos u \sum_{n=-\infty}^{\infty} \delta \left(\frac{1}{4} \frac{t}{T} - n \right) \right\}.^3 \quad (1.3.14)$$

For $K = 0$, the map (1.3.5), or (1.3.7), describes a pure rotation as opposed to the standard map (1.2.8). This renders both maps quite

³It is shown in [D 95] that an exact relationship exists between \hat{M}_4 and \hat{M}_H .

different from each other. To view it, rewrite the Hamiltonian (1.3.1) by using the action-angle variables:

$$P = (2I\omega_0)^{1/2} \cos \phi, \quad x = (2I/\omega_0)^{1/2} \sin \phi. \quad (1.3.15)$$

After substituting (1.3.15) in (1.3.1), one derives

$$H = \omega_0 I - \frac{\omega_0}{T} K \cos[(2I/\omega_0)^{1/2} \sin \phi] \sum_{n=-\infty}^{n+\infty} \delta\left(\frac{t}{T} - n\right). \quad (1.3.16)$$

The unperturbed Hamiltonian in (1.2.1) is $H_0 = \frac{1}{2}I^2$ and the corresponding frequency satisfies the condition

$$\frac{d\omega(I)}{dI} = \frac{d^2 H_0}{dI^2} \neq 0 \quad (1.3.17)$$

while in the case of (1.3.16), $H_0 = \omega_0 I$ and

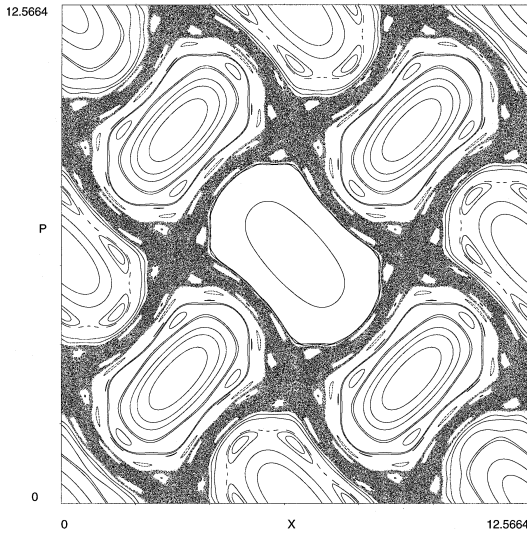
$$\frac{d\omega(I)}{dI} = 0, \quad (1.3.18)$$

which indicates the existence of degeneracy. Hence the standard map and the web-map complement each other in various physical situations.

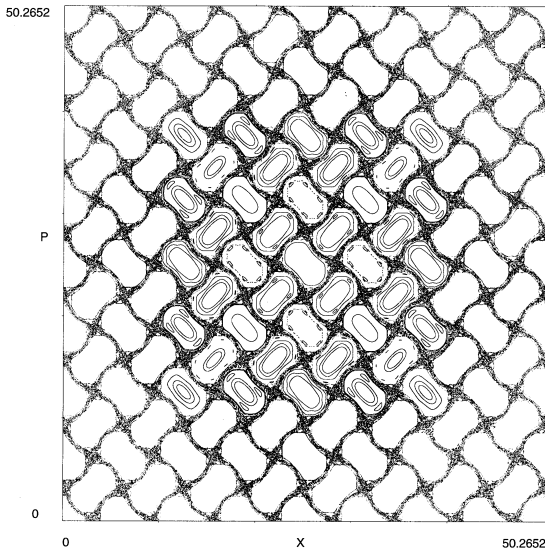
Another important property of the web-map (1.3.5) is that it can be considered a dynamical generator of the q -fold symmetry for the resonance condition (1.3.9), which is of the crystalline type for

$$q \in \{q_c\} = \{1, 2, 3, 4, 6\} \quad (1.3.19)$$

and the quasi-crystal type for $q \notin \{q_c\}$. This topic will be discussed in greater detail in Chapter 8. A fundamental domain exists for (1.3.19). Examples of a phase plane with narrow stochastic layers are given in Fig. 1.3.1 for $q = 4$ and Fig. 1.3.2 for $q = 3$ and 6. These illustrations demonstrate the existence of the stochastic web of a corresponding symmetry in the phase plane. The stochastic web is a net with each part being a stochastic layer. One can say that the net of channels, which constitute the stochastic web, provides particle transport along the web. The stochastic web can be finite or infinite. The issues related to it will be discussed in Chapter 8.

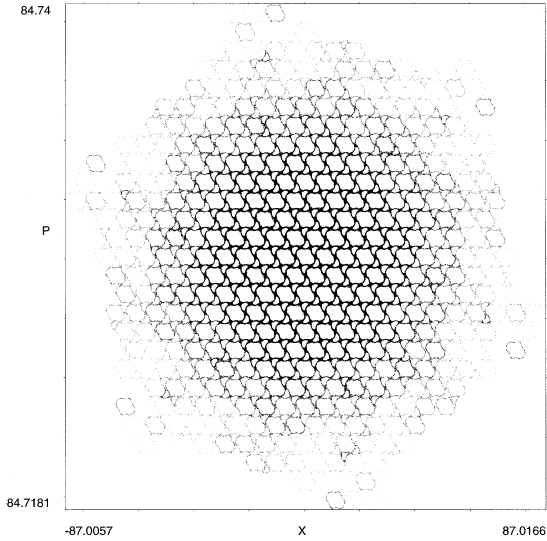


(a)

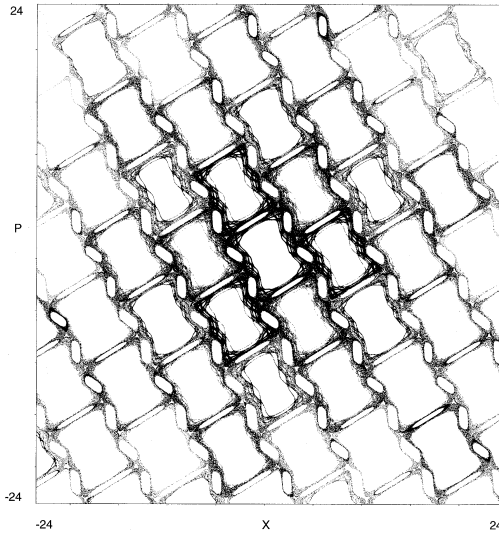


(b)

Fig. 1.3.1. Stochastic web and invariant curves for the four-fold symmetry ($q = 4$, $K = 1.5$): (a) element of the web; (b) magnification of the central part of the web.



(a)



(b)

Fig. 1.3.2. Random walk along the stochastic web with: (a) $q = 6$, $K = 1.2$; (b) $q = 3$, $K = 1.7$.

1.4 Perturbed Pendulum

The perturbed pendulum is a typical model of the continuous equation of motion (no kicks) where one can still introduce a map. The Hamiltonian of the model is

$$H = \frac{1}{2}\dot{x}^2 - \omega_0^2 \cos x + \epsilon\omega_0^2 \cos(kx - \nu t). \quad (1.4.1)$$

Here ω_0 is the frequency of small oscillations in the unperturbed pendulum with Hamiltonian

$$H_0 = \frac{1}{2}\dot{x}^2 - \omega_0^2 \cos x, \quad (1.4.2)$$

where ϵ is the small dimensionless parameter of perturbation and ν the frequency of perturbation. The Hamiltonian (1.4.1) corresponds to the pendulum (1.4.2) with rotating point of suspension.⁴ The following equation of motion describes the perturbed pendulum:

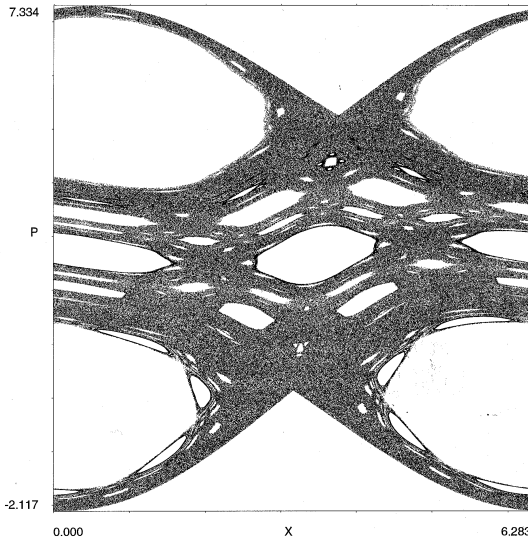
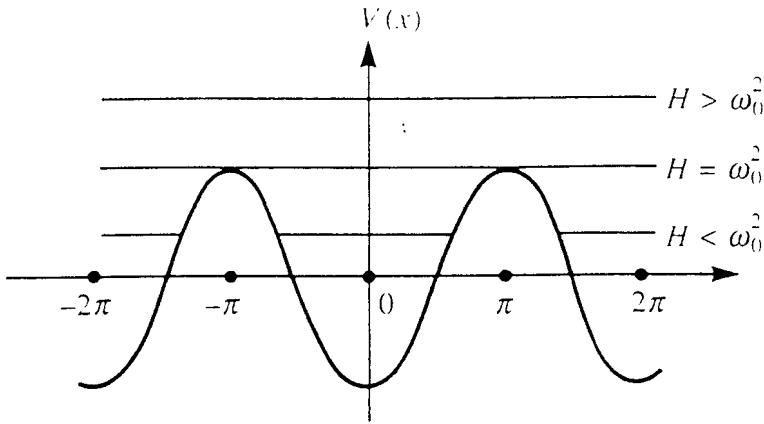
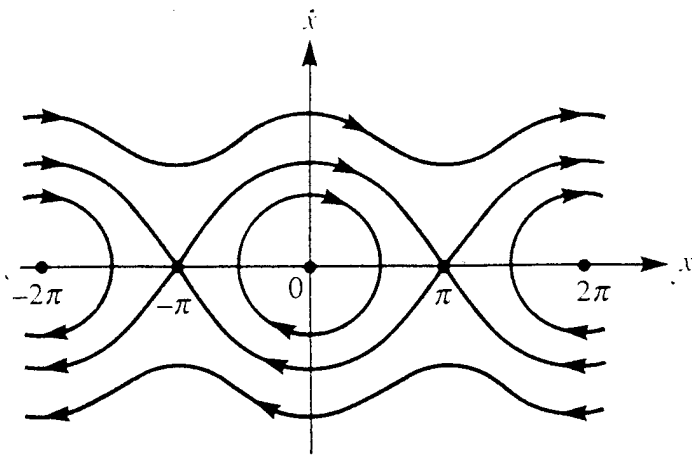


Fig. 1.4.1. Area of chaotic dynamics for the perturbed pendulum. All points belong to the only trajectory ($\epsilon = 0.9$; $\nu = 5.4$).

⁴See [LL 76] for the corresponding derivation of the Lagrangian in the model.



(a)



(b)

Fig. 1.4.2. Unperturbed pendulum: (a) periodic potential; (b) the phase portrait.

$$\ddot{x} + \omega_0^2 \sin x = \epsilon k \omega_0^2 \sin(kx - \nu t). \tag{1.4.3}$$

The Poincaré map can be considered as a set of trajectory points (x, \dot{x}) on the phase plane taken at each period $T = 2\pi/\nu$ of perturbation. Figure 1.4.1 exemplifies the complexity of the corresponding dynamics.

The problem of (1.4.3) will be considered in Chapter 2. A good knowledge of unperturbed pendulum dynamics is required. The phase portrait of the pendulum (1.4.2) is shown in Fig. 1.4.2. Its main feature is the existence of a separatrix at the energy

$$H_0 = H_s = \omega_0^2 \quad (1.4.4)$$

with a corresponding solution for the co-ordinate

$$x = 4 \arctan \exp(\pm \omega_0 t) - \pi \quad (1.4.5)$$

(it has a form called a “kink”) and for the momentum p or velocity if the mass is equal to one,

$$p = v = \dot{x} = \pm \frac{2\omega_0}{\cosh \omega_0 t}, \quad (1.4.6)$$

which is called a “soliton”. The necessary information on the pendulum is presented in Appendix 1 where the action-angle variables (I, θ) defined by the relations

$$\begin{aligned} I &= \frac{1}{2\pi} \oint p dx \\ \theta &= \frac{\partial S(x, I)}{\partial I} = \frac{\partial}{\partial I} \int^x dp x \end{aligned} \quad (1.4.7)$$

with

$$p = \pm [2(H_0 + \omega_0^2 \cos x)]^{1/2} \quad (1.4.8)$$

are used.

The integration in the definition of I is performed over the period of motion $2\pi/\omega(I)$ where the nonlinear frequency

$$\omega(I) = dH_0(I)/dI \quad (1.4.9)$$

is introduced and the condition $H_0 < \omega_0^2$ is applied. In the case of $H_0 \geq \omega_0^2$, the integration in (1.4.7) is performed over the interval $x \in (0, 2\pi)$ for both positive and negative p . The details are found in Appendix 1.

Instead of using $\omega(I)$, it is sometimes convenient to use $\omega(H_0)$ and the connection, $I = I(H_0)$, which follows from (1.4.7).

As will be clearly seen in Chapter 2, the time dependence of the velocity \dot{x} in the vicinity of the unperturbed separatrix is crucial to the problem (1.4.1) (see also (A.1.11)). This dependence is shown in Fig. 1.4.3 for $H_0 < H_s$. It resembles a periodic set of kicks that makes it possible to define the so-called separatrix map, the definition of which can be found in Section 2.3. The importance of the perturbed pendulum model (1.4.1) lies in its universality in studying the separatrix destruction.

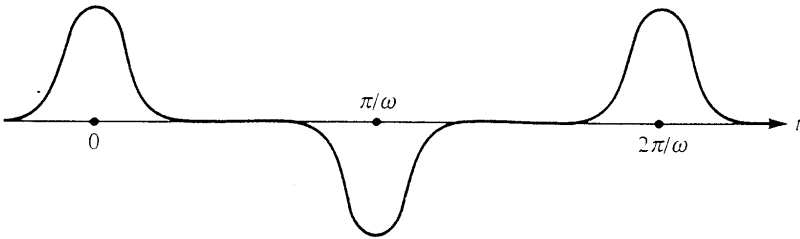


Fig. 1.4.3. The pendulum velocity in the vicinity of separatrix as a function of time.

1.5 Perturbed Oscillator

For fairly small amplitudes of oscillations, the pendulum equation can be reduced to the linear oscillator equation and the problem (1.4.1) replaced by the perturbed oscillator problem with Hamiltonian

$$H = \frac{1}{2}(\dot{x}^2 + \omega_0^2 x^2) + \epsilon \frac{\omega_0^2}{k^2} \cos(kx - \nu t) \quad (1.5.1)$$

and the equation of motion

$$\ddot{x} + \omega_0^2 x = \frac{1}{k} \epsilon \omega_0^2 \sin(kx - \nu t). \quad (1.5.2)$$

Problem (1.5.2) has another physical interpretation. It is equivalent to the motion of a particle in a constant magnetic field, B_0 , and in the field of a plane wave travelling perpendicularly to the magnetic field. In this case, the equation of motion of a particle is written as

$$\ddot{\mathbf{r}} = \frac{e}{mc} [\dot{\mathbf{r}}, \mathbf{B}_0] + \frac{e}{m} \mathbf{E}_0 \sin(\mathbf{k}\mathbf{r} - \nu t), \quad (1.5.3)$$

where $[\cdot, \cdot]$ means vector product. Assuming that \mathbf{B}_0 is directed along the z -axis, the vector \mathbf{r} lies in the plane (x, y) , and vectors \mathbf{k} and \mathbf{E}_0 are directed along the x -axis (a longitudinal wave), it follows from (1.5.3) that

$$\begin{aligned} \ddot{x} &= \omega_0 \dot{y} + \frac{1}{k} \epsilon \omega_0^2 \sin(kx - \nu t), \\ \ddot{y} &= -\omega_0 \dot{x}, \end{aligned} \quad (1.5.4)$$

where

$$\omega_0 = eB_0/mc, \quad \epsilon \omega_0^2 = eE_0 k/m. \quad (1.5.5)$$

From (1.5.4), it follows that the existence of an integral of motion is

$$\dot{y} + \omega_0 x = \text{const}. \quad (1.5.6)$$

Assuming that $\text{const} = 0$, we arrive at Eq. (1.5.2).

System (1.5.1) possesses the same degeneracy property in its unperturbed part as the kicked-pendulum case (1.3.1). As in (1.3.15), we can introduce the action-angle variables (I, ϕ) :

$$\begin{aligned} \dot{x} &= (2\omega_0 I)^{1/2} \cos \phi, \\ x &= (2I/\omega_0)^{1/2} \sin \phi. \end{aligned} \quad (1.5.7)$$

Expressed via the following variables, the Hamiltonian (1.5.1) is

$$H = \omega_0 I + \epsilon V(I, \phi; t), \quad (1.5.8)$$

$$V(I, \phi; t) = \frac{1}{k^2} \omega_0^2 \cos \left[k \left(\frac{2I}{\omega_0} \right)^{1/2} \sin \phi - \nu t \right].$$

The unperturbed part of the Hamiltonian, $H_0 = \omega_0 I$, does not satisfy the non-degeneracy condition (1.3.17). Therefore, in the case of a resonance

$$n\omega_0 = \nu, \quad (1.5.9)$$

where n is an integer, the amplitude of the oscillator increases strongly.

Chapter 2 will demonstrate that the degeneracy of the unperturbed Hamiltonian causes a stochastic web to be generated in the phase space of a system when affected by a periodic perturbation.

1.6 Billiards

A system involving a point-size ball bouncing between different scatterers with elastic collisions is called a billiard. An example of a Sinai

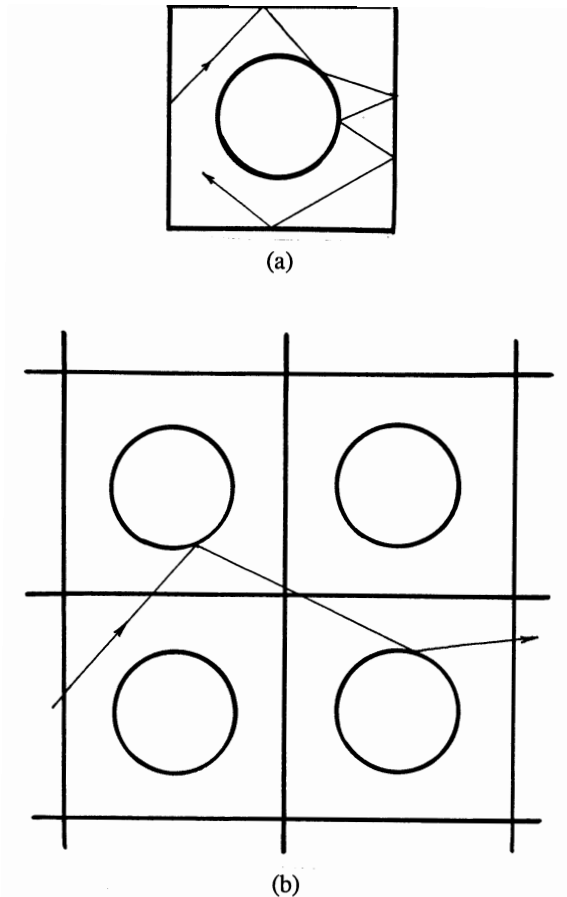


Fig. 1.6.1. Sinai billiard (a) and its double-periodic continuation (b).

billiard is shown in Fig. 1.6.1(a). The figure can be considered a fundamental domain and it can be periodically continued in x -, y - or in both directions, as shown in Fig. 1.6.1(b). In the latter case, it is called Lorentz gas. The dynamics of a particle (ball) in a two-dimensional billiard can be described using two canonical pairs of variables $(x, v_x; y, v_y)$. In reality, a conservation law,

$$v_x^2 + v_y^2 = \text{const} = 1, \quad (1.6.1)$$

exists due to the elasticity of collisions. This property makes it possible to use a two-dimensional map linking one collision to the next:

$$(x_{n+1}, v_{x,n+1}) = \hat{T}_x(x_n, v_{x,n}) \quad (1.6.2)$$

or

$$(y_{n+1}, v_{y,n+1}) = \hat{T}_y(y_n, v_{y,n}). \quad (1.6.3)$$

Both of the above equations are equivalent, and points x or y can be obtained from the fundamental domain. There is also another type of map which considers the point of collision using the inner scatterer and its corresponding velocity. All maps are area-preserving since the system is Hamiltonian.

Billiards can be considered one of the most attractive types of dynamical models in the study of ergodic and mixing properties in Hamiltonian systems. A particle in a billiard with absolute elastic collisions was used to analyse the origin of statistical laws. There are different physical problems and whose study can be reduced to a billiard-type problem. One of them is ray propagation in non-uniform waveguides.⁵

The geometry of the billiard model defines a particular type of chaos and an order for the trajectories. For instance, the scatterer in the ‘‘Cassini billiard’’ has the shape of the Cassini’s oval:

$$(x^2 + y^2)^2 - 2c^2(x^2 - y^2) - (a^4 - c^4) = 0. \quad (1.6.4)$$

⁵Ray dynamics can be written in a Hamiltonian form. Reflecting rays from the waveguide walls render the problem similar to the billiard problem. One can find out more on ray chaos in [AZ 91] and [Ab 91].

The shape of the oval is sensitive to the parameters a and c and can have both concave and convex parts. The phase space of the Cassini billiard is much more complicated than that of the Sinai billiard since it permits a non-ergodic motion due to the islands in the phase space. One can also consider an analog of the Lorentz gas if a double-periodic continuation of the scatterers is made (see Fig. 1.6.2). The concave part of the scatterer's boundary makes it possible to trap the trajectories for an arbitrarily long (but finite) time.

The specific properties of the billiards are discussed in Sections 7.3 and 7.4.

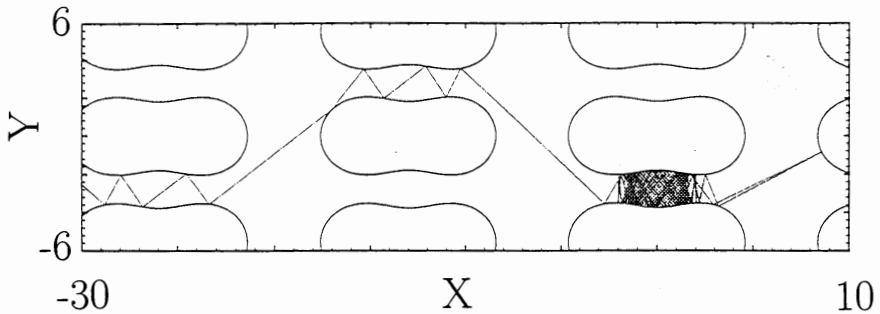


Fig. 1.6.2. Example of a trajectory in the Cassini billiard (with double-periodic continuation).

Conclusions

1. One can select a special set of time instants, $\{t_j\} = \{t_1, t_2, \dots\}$, and find the dependence of system co-ordinates and moments, $(\mathbf{p}_{n+1}, \mathbf{q}_{n+1})$, at time t_{n+1} as a function of the co-ordinates and moments $(\mathbf{p}_n, \mathbf{q}_n)$ at time t_n . The corresponding time shift operator \hat{T}_n

$$\hat{M}: (\mathbf{p}_{n+1}, \mathbf{x}_{n+1}) = \hat{T}_n(\mathbf{p}_n, \mathbf{x}_n)$$

defines the Poincaré map \hat{M} . The conveniently taken set, $\{t_j\}$, can help, that is, the investigation of the properties of the map \hat{M} is easier than a study of the initial equation of motion. Any map \hat{M} is area-preserving for Hamiltonian systems (it is equivalent to the Liouville theorem on the phase volume conservation).

2. There are few models of maps which are carriers of typical properties of physical systems. The most popular model is the standard map,

$$\hat{M}_{\text{st}}: \begin{aligned} p_{n+1} &= p_n + K \sin x_n \\ x_{n+1} &= x_n + p_{n+1}, \end{aligned}$$

which corresponds to a periodically kicked rotator. An alternative to map \hat{M}_s , with respect to some important condition of degeneracy, is the web-map,

$$\hat{M}_\alpha: \begin{aligned} u_{n+1} &= (u_n + K \sin v_n) \cos \alpha + v_n \sin \alpha \\ v_{n+1} &= -(u_n + K \sin v_n) \sin \alpha + v_n \cos \alpha, \end{aligned}$$

which generates stochastic webs for $\alpha = 2\pi/q$ with integer $q > 2$. The map \hat{M}_α corresponds to a periodically kicked oscillator.

3. Billiard-type systems naturally generate a map to connect variables that correspond to two continuous reflections of a ball. The set $\{t_j\}$ is not periodic for maps in billiard-type systems.
4. It is not easy to find a map-form corresponding to the equations of motion for typical physical systems, such as the perturbed oscillator or pendulum. We are lucky when that happens.